Supporting Information for

A PET radiotracer for imaging macrophage colony-stimulating factor 1 receptor (CSF-1R) in neuroinflammation

Andrew G. Horti[1]*, Ravi Naik[1], Catherine Foss[1], Il Minn[1], Varvara Misheneva[2], Yong Du[1], Yuchuan Wang[3], William B. Matthews[1], Yunkou Wu[1], Andrew Hall[1], Catherine LaCourse[2], Hye-Hyun Ahn[1], Hwanhee Nam[1], Wojciech Lesniak[1], Heather Valentine[1], Olga Pletnikova[3], Juan Troncoso[3], Matthew Smith[4], Peter Calabresi[4], Alena Savonenko[5], Robert F. Dannals,[1] Mikhail V. Pletnikov[2], Martin G. Pomper[1]*

Russell H. Morgan Departments of Radiology[1], The Johns Hopkins University School of Medicine, 600 North Wolfe Street, Baltimore, MD 21287-0816, USA; [3]Merck & Co., Kenilworth, NJ 07033, USA

INTRODUCTION

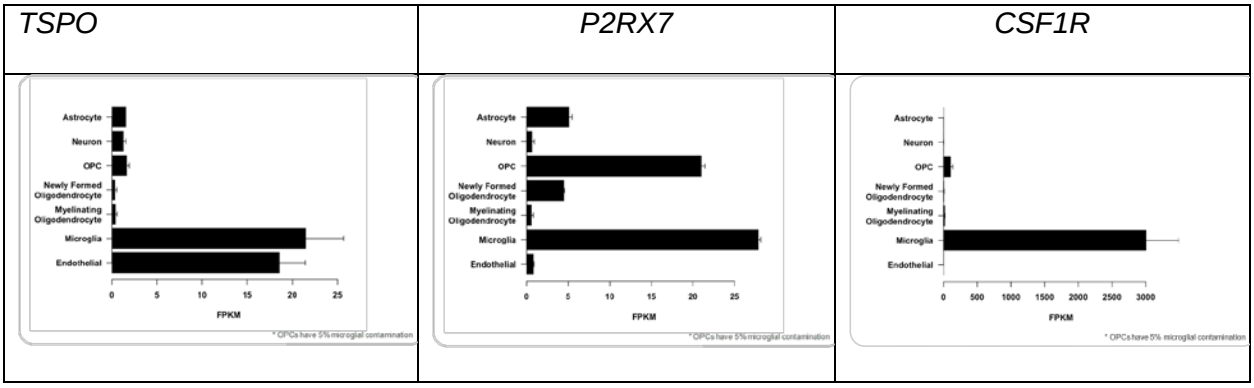

Figure S1. In the CNS cells the *CSF1R* gene is mainly expressed in microglia, whereas *TSPO* and *P2RX7* genes exhibit multi-cellular expression. Abbreviators: OPC = Oligodendrocyte progenitor cells; FPKM = fragments per kilobase of transcript per million mapped reads. The graphs are copied from the http://web.stanford.edu/group/barres_lab/brain_rnaseq.html website.

MATERIALS AND METHODS

CSF1R inhibitors: BLZ945 (1) was purchased from AstaTech (Bristol, PA), pexidartinib (PLX3397) (2) from eNovation Chemicals (Bridgewater, NJ) and compound 8 was prepared in-house as described previously (3).

Chemistry: ^{1}H NMR spectra were recorded with a Bruker-500 NMR spectrometer at nominal resonance frequencies of 500 MHz in $CDCl_3$, CD_3OD or DMSO-d_6 (referenced to internal Me_4Si at δ 0 ppm). High-resolution mass spectra were recorded commercially utilizing electrospray ionization (ESI) at the University of Notre Dame Mass Spectrometry facility.

Synthesis of 5-Cyano-*N*-(4-(4-methylpiperazin-1-yl)-2-(piperidin-1-yl)phenyl)furan-2-carboxamide (CPPC) was performed as described elsewhere (3).

1-(5-Chloro-2-nitrophenyl)piperidine: To a cooled (0 ^{0}C) solution of 1.0 g (10.0 mmol) of 4-chloro-2-fluoronitrobenzene in 15 mL of EtOH was added 1.7 mL (30.0 mmol) of piperidine dropwise over 5 min. The solution stirred at 0 °C for 10 min and then at 23 ^{0}C for 30 min. The mixture was poured into water (225 mL) and extracted with EtOAc (2 x 30 mL). The combined extracts were washed with saturated aq $NaHCO_3$ and brine (30 mL each) and then dried over Na_2SO_4 and evaporated to get the crude compound. The resulting residue was purified by silica gel column chromatography (Hexane:EtOAc = 9.5:0.5) to give 1-(5-chloro-2-nitrophenyl)piperidine as a yellow solid (1.32 g, 96% yield). ^{1}H NMR (500 MHz, $CDCl_3$) δ 7.77 (d, *J* = 5.0 Hz, 1H), 7.13 (s, 1H), 6.93 (d, *J* = 10.0 Hz, 1H), 3.30–3.27 (m, 2H), 2.91–2.86 (m, 2H), 1.90–1.86 (m, 1H), 1.75–1.73 (m, 2H), 1.49–1.42 (m, 1H).

1-Methyl-4-(4-nitro-3-(piperidin-1-yl)phenyl)piperazine: A mixture of 1-(5-chloro-2-nitrophenyl)piperidine (1.0 g, 4.15 mmol) and 1-methylpiperazine (1.38 mL, 12.46 mmol) were heated with stirring under N_2 at 138 °C for 12h. After cooling to rt, the mixture was poured into

water and extracted with ethyl acetate (2 x 100 mL). The combined extracts were washed with water and brine and then dried over Na_2SO_4 and evaporated to get the crude compound. The resulting residue was purified by silica gel column chromatography (CH_2Cl_2: MeOH = 9:1) to give 1-methyl-4-(4-nitro-3-(piperidin-1-yl)phenyl)piperazine as a yellow solid (1.2 g, 96% yield). ^{1}H NMR (500 MHz, $CDCl_3$) δ 7.62 (d, *J* = 5.0 Hz, 1H), 6.80 (s, 1H), 6.43 (d, *J* = 10.0 Hz, 1H), 3.84 (t, *J* = 5.0 Hz, 4H), 3.71 (t, *J* = 5.0 Hz, 2H), 3.60 (t, *J* = 5.0 Hz, 4H), 3.50 (d, *J* = 10.0 Hz, 2H), 3.80 (d, *J* = 5.0 Hz, 2H), 1.55–1.51 (m, 3H).

4-(4-methylpiperazin-1-yl)-2-(piperidin-1-yl)aniline: To a mixture of 1-methyl-4-(4-nitro-3-(piperidin-1-yl)phenyl)piperazine (1.2 g, 3.94 mmol), and NH_4Cl (2.10 g, 39.4 mmol) in THF/MeOH/H_2O (10:5:3) (20 mL), was added Zn dust (2.57 g, 39.4 mmol) at 90 ˚C, then the mixture was refluxed for 1 h. After completion of the reaction, the reaction mixture was filtered through Celite and partitioned between EtOAc and brine. The organic layer was separated, dried over anhydrous $MgSO_4$, filtered, and concentrated *in vacuo*. The resulting residue was purified by silica gel column chromatography (CH_2Cl_2: MeOH = 9:1) to give 4-(4-methylpiperazin-1-yl)-2-(piperidin-1-yl)aniline as a brown solid (0.98 g, 90.7% yield).

5-Cyano-*N*-(4-(4-methylpiperazin-1-yl)-2-(piperidin-1-yl)phenyl)furan-2-carboxamide (CPPC): To the mixture of 4-(4-methylpiperazin-1-yl)-2-(piperidin-1-yl)aniline (0.5 g, 1.82 mmol), 5-cyanofuran-2-carboxylic acid (0.3 g, 2.18 mmol), HATU (0.83 g, 2.18 mmol), in DMF (10 mL) was added DIPEA (0.63 mL, 3.64 mmol). The reaction mixture was stirred at room temperature overnight and then partitioned between EtOAc and brine. The organic layer was separated, dried over anhydrous $MgSO_4$, filtered, and concentrated under a vacuum. The resulting residue was purified by silica gel column chromatography (CH_2Cl_2: MeOH = 9:1) to give 5-cyano-N-(4-(4-methylpiperazin-1-yl)-2-(piperidin-1-yl)phenyl)furan-2-carboxamide as a yellow solid (0.6g, 84.5% yield). ^{1}H NMR (500 MHz, $CDCl_3$) δ 9.53 (s, 1H), 8.31 (d, *J* = 8.7 Hz, 1H), 7.23 (d, *J* = 16.6 Hz, 2H), 6.80 (s, 1H), 6.72 (d, *J* = 8.8 Hz, 1H), 3.20 (s, 4H), 2.85 (s, 4H), 2.59 (s, 4H), 2.36 (s, 3H),

1.80 (s, 4H), 1.65 (s, 2H). HRMS calculated for C22H28N5O2 ([M + H)] 394.223752, found 394.223065.

Synthesis of 5-Cyano-*N*-(4-(piperazin-1-yl)-2-(piperidin-1-yl)phenyl)furan-2-carboxamide (Pre-CPPC)

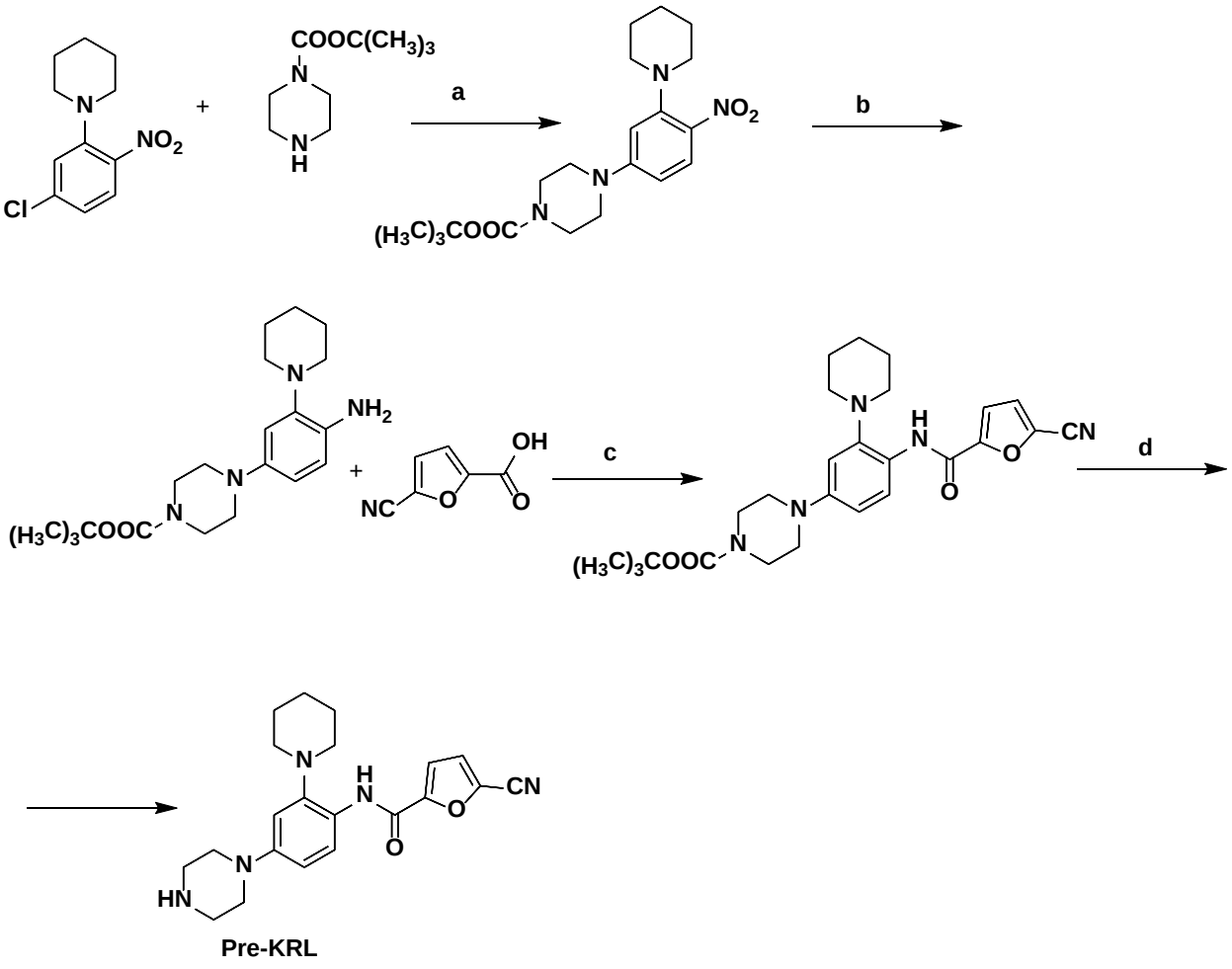

Figure S2. Synthesis of Pre-CPPC.

Step a. *Tert-butyl* 4-(4-nitro-3-(piperidin-1-yl)phenyl)piperazine-1-carboxylate: To the mixture of 1-(5-chloro-2-nitrophenyl)piperidine (1.0 g, 4.15 mmol) and *tert*-butyl piperazine-1-carboxylate (1.55 g, 8.30 mmol), in DMSO (10 mL) was added K_2CO_3 (1.72 g, 12.45 mmol). The

reaction mixture was stirred at 110 °C for 12h and then partitioned between EtOAc and brine. The organic layer was separated, dried over anhydrous $MgSO_4$, filtered, and concentrated under a vacuum. The resulting residue was purified by silica gel column chromatography (Hexane:EtOAc = 3:7) to give *tert*-butyl 4-(4-nitro-3-(piperidin-1-yl)phenyl)piperazine-1-carboxylate as a white solid (1.40 g, 86.4% yield). ^{1}H NMR (500 MHz, $CDCl_3$) δ 7.99 (d, *J* = 10.0 Hz, 1H), 6.38 (d, *J* = 10.0 Hz, 1H), 6.31 (s, 1H), 3.58 (t, *J* = 5.0 Hz, 4H), 3.34 (t, *J* = 5.0 Hz, 4H), 2.28 (t, *J* = 5.0 Hz, 2H), 2.78 (d, *J* = 10.0 Hz, 2H), 1.70 (d, *J* = 5.0 Hz, 2H), 1.55–1.51 (m, 3H), 1.47 (s, 9H).

Step b. *Tert*-butyl 4-(4-amino-3-(piperidin-1-yl)phenyl)piperazine-1-carboxylate: To a mixture of *tert*-butyl 4-(4-nitro-3-(piperidin-1-yl)phenyl)piperazine-1-carboxylate (1.20 g, 3.07 mmol), and NH_4Cl (1.64 g, 30.7 mmol) in THF/MeOH/H_2O (10:5:3) (20 mL), was added Zn dust (2.0 g, 30.7 mmol) at 90 ˚C, then the mixture was refluxed for 1 h. After completion of the reaction, the reaction mixture was filtered through Celite and partitioned between EtOAc and brine. The organic layer was separated, dried over anhydrous $MgSO_4$, filtered, and concentrated *in vacuo*. The resulting residue was purified by silica gel column chromatography (CH_2Cl_2: MeOH = 9:1) to give *tert*-butyl 4-(4-amino-3-(piperidin-1-yl)phenyl)piperazine-1-carboxylate as a brown solid (1.0 g, 90.3% yield).

Step c. *Tert*-butyl 4-(4-(5-cyanofuran-2-carboxamido)-3-(piperidin-1-yl)phenyl)piperazine-1-carboxylate: To the mixture of *tert*-butyl 4-(4-amino-3-(piperidin-1-yl)phenyl)piperazine-1-carboxylate (0.5 g, 1.38 mmol), 5-cyanofuran-2-carboxylic acid (0.23 g, 1.66 mmol), HATU (0.63 g, 1.66 mmol), in DMF (10 mL) was added DIPEA (0.48 mL, 2.76 mmol). The reaction mixture was stirred at room temperature overnight and then partitioned between EtOAc and brine. The organic layer was separated, dried over anhydrous $MgSO_4$, filtered, and concentrated under a vacuum. The resulting residue was purified by silica gel column chromatography (CH_2Cl_2: MeOH = 9:1) to give *tert*-butyl 4-(4-(5-cyanofuran-2-carboxamido)-3-(piperidin-1-yl)phenyl)piperazine-1-carboxylate as a yellow solid (0.60 g, 90.9% yield). ^{1}H NMR

(500 MHz, $CDCl_3$) δ 9.59 (s, 1H), 8.31 (d, *J* = 5.0 Hz, 1H), 7.25 (d, *J* = 5.0 Hz, 1H), 7.21 (d, *J* = 5.0 Hz, 1H), 6.79 (s, 1H), 6.72 (d, *J* = 5.0 Hz, 1H), 3.58 (t, *J* = 5.0 Hz, 4H), 3.10 (t, *J* = 5.0 Hz, 4H), 2.99 (t, *J* = 5.0 Hz, 2H), 2.72 (t, *J* = 10.0 Hz, 2H), 1.83 (d, *J* = 10.0 Hz, 2H), 1.55–1.51 (m, 3H), 1.49 (s, 9H).

Step d. 5-Cyano-*N*-(4-(piperazin-1-yl)-2-(piperidin-1-yl)phenyl)furan-2-carboxamide (Pre-CPPC): To a solution of *tert*-butyl 4-(4-(5-cyanofuran-2-carboxamido)-3-(piperidin-1-yl)phenyl)piperazine-1-carboxylate (0.5 g, 1.04 mmol) in methylene chloride (5 mL) was added trifluoroacetic acid (0.39 mL, 5.21 mmol) dropwise at 0 °C, and then, the mixture was stirred at room temperature for 12 h. After completion of the reaction, the reaction mixture was concentrated under reduced pressure. The resulting residue was purified by silica gel column chromatography (CH_2Cl_2: MeOH = 9:1) to give 5-cyano-*N*-(4-(piperazin-1-yl)-2-(piperidin-1-yl)phenyl)furan-2-carboxamide as a pale yellow solid (0.3 g, 76.0% yield). ^{1}H NMR (500 MHz, $CDCl_3$) δ 9.60 (s, 1H), 8.31 (d, *J* = 5.0 Hz, 1H), 7.25 (d, *J* = 5.0 Hz, 1H), 7.21 (d, *J* = 5.0 Hz, 1H), 6.79 (s, 1H), 6.72 (d, *J* = 5.0 Hz, 1H), 3.15 (t, *J* = 5.0 Hz, 4H), 3.08 (t, *J* = 5.0 Hz, 4H), 2.99 (t, *J* = 5.0 Hz, 2H), 2.73 (t, *J* = 10.0 Hz, 2H), 1.84 (d, *J* = 10.0 Hz, 2H), 1.57 (s, 1H), 1.55–1.51 (m, 3H); HRMS calculated for C21H26N5O2 ([M + H)] 380.208102, found 380.207980

Radiosynthesis of [^{11}C]CPPC (Fig. S3).

To a 1 mL V-vial, Pre-CPPC (1 mg) was added to 0.2 mL of anhydrous DMF. [^{11}C]Methyl iodide, carried by a stream of helium, was trapped in the above mentioned solution. The reaction was heated in 80°C for 3.5 min, then quenched with 0.2 mL of water. The crude reaction product was purified by reverse-phase high performance liquid chromatography (HPLC) at a flow rate of 12 mL/min. The radiolabeled product (t_R = 6.5-7.2 min) that was fully separated from the precursor (t_R = 2.5 min) was remotely collected in a solution of 0.3 g sodium ascorbate in a mixture of 50 mL water with 1 mL 8.4% aq. $NaHCO_3$. The aqueous solution was transferred through an

activated Waters Oasis Sep-Pak light cartridge (Milford, MA). After washing the cartridge with 10 mL saline, the product was eluted with 1 mL of ethanol through a 0.2 μM sterile filter into a sterile, pyrogen-free vial and 10 mL of 0.9% saline was added through the same filter. The final product, [^{11}C]CPPC, was analyzed by analytical HPLC to determine the radiochemical purity and specific radioactivity.

HPLC conditions. Preparative: Column, XBridge C18, 10x250 mm (Waters, Milford, MA). Mobile phase: 45%:55% acetonitrile:triethylamine-phosphate buffer, pH 7.2. Flow rate: 12 mL/min, retention time 7 min. Analytical: Column, Luna C18, 10 micron, 4.6x250 mm (Phenomenex, Torrance, CA). Mobile phase: 60%:40% acetonitrile:0.1M aq. ammonium formate. Flow rate: 3 mL/min, retention time 3.5 min.

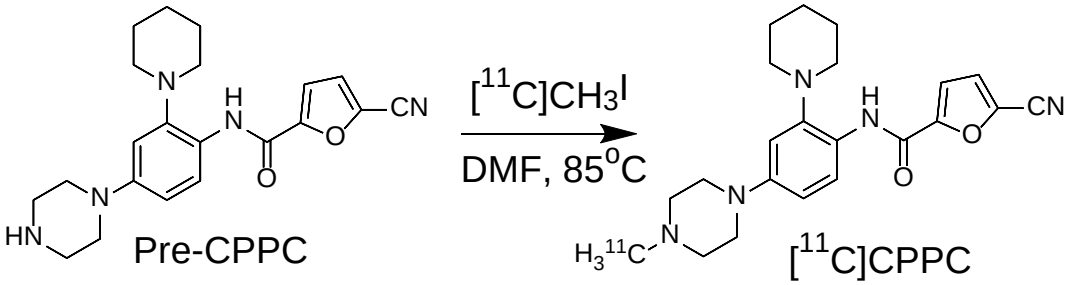

Figure S3. Radiosynthesis of [^{11}C]CPPC.

Biodistribution and PET imaging studies with [^{11}C]CPPC in mice.

Table S1. Summary of [^{11}C]CPPC biodistribution and other studies in mice

detailed methods, SI page number	Study	Mice (number of animals)	Blocker (doses)	Figure or Table
10	Controls, Baseline	C57BL/6J (3 per time point; Total: 12)	-	Table S2
11	Controls, blocking - dose escalation	CD1 (5 per dose; Total: 30)	CPPC (0 – 20 mg/kg, IP)	Fig. S4
12 - 13	Controls, baseline *vs* blocking, without blood (Fig. S5A) and with blood correction (Fig. S5B)	CD1 (3 per group; Total: 9)	CPPC (0, 0.6 or 3.0 mg/kg; IP)	Fig. S5
14-15	Controls vs microglia-depleted	C57BL/6J (5 per group; 10 total)	PLX3397 (290 mg/kg chow)	Fig. S6A
14-15	Controls vs CSF1R-KO	Controls - C57BL/6J (5). CSF1R-KO - B6.Cg-Csf1r$^{tm1.2Jwp}$/J (5) Total: 10	-	Fig. S6B
16	Controls vs LPS (intracranial) Experiment 1	Sham baseline – CD1 (3) LPS baseline – CD1 (3) LPS block – CD1 (3) Total: 9	CPPC (0.3 mg/kg, IP)	Fig. 1A
16 - 17	Controls vs LPS (intracranial) Experiment 2	Sham – CD1 (4) LPS baseline – CD1 (4) LPS block-1 – CD1 (4) LPS block-2 – CD1 (4) Total mice: 16	Block-1: CPPC (0.6 mg/kg, IP) Block-2: CPPC (1.2 mg/kg, IP)	Fig. 1B
18	Controls vs LPS (IP) Experiment 1	Controls - CD1 (5), IP LPS mice baseline – CD1 (5) IP LPS mice blocking – CD1 (5) Total mice: 15	CPPC (1 mg/kg, IP)	Fig. 2A
18 - 19	Controls vs LPS (IP) Experiment 2	Controls - CD1 (5), IP LPS mice baseline – CD1 (5) IP LPS mice blocking – CD1 (5) Total mice: 15	CPPC (1 mg/kg, IP)	Fig. 2B

19	Controls vs LPS (IP) Experiment 3	Controls - CD1 (3), IP LPS mice baseline – CD1 (6) IP LPS mice blocking – CD1 (6) Total mice: 15	Compound 8 (2 mg/kg, IP)	Fig. 2C
20	Controls vs Alzheimer's mouse model	Controls – (6) Transgenic APP - (6) Total mice: 12	-	Fig. 3
21 - 23	Full body radiation dosimetry	CD1 (3 per time point) Total: 15	-	Table S3
24 - 25	PET/CT, EAE mice	EAE mice (3) Control (1) Total: 4	-	Fig. 4, Fig. S7
26	Radiometabolites in mouse plasma and brain	CD1 (3 per time point) Total: 6	-	Table S4
27 - 28	PCR and Western blot of LPS mouse brains	Controls – CD1 (6) LPS i.p. treated – CD1 (6) Total: 12	-	Fig. S8

Brain regional distribution of [^{11}C]CPPC in normal control mice, baseline: Male C57BL/6J mice of four to eight weeks of age, weighing 22-24 g from Charles River Laboratories (Wilmington, MA) were used. Animals were sacrificed by cervical dislocation at at 5, 15, 30 and 60 min (3 mice per time-point) following injection of 5.6 MBq (0.15 mCi) [11C]CPPC [specific radioactivity = 462 GBq/μmol (12.5 Ci/μmol)] in 0.2 mL saline into a lateral tail vein. The brains were removed and dissected on ice. The brain regions (cerebellum, olfactory bulbs, hippocampus, frontal cortex, brain stem and rest of brain) were weighed and their radioactivity content was determined in a γ-counter LKB/Wallac 1283 CompuGamma CS (Bridgeport, CT). The percentage of standardized uptake value (%SUV) was calculated (Table S2).

Table S2. Regional brain distribution of [^{11}C]CPPC in control mice after radiotracer injection: SUV ± SD (n = 3)

	5 min	15 min	30 min	60 min
Cerebellum	138 ± 9	110 ± 17	70 ± 4	71 ± 3
Olfactory bulbs	142 ± 12	124 ± 21	86 ± 9	90 ± 3
Hippocampus	124 ± 4	121 ± 25	94 ± 12	95 ± 3
Frontal Cortex	147 ± 8	150 ± 30	102 ± 16	107 ± 8
Brain stem	120 ± 19	106 ± 17	75 ± 11	79 ± 3
Rest of brain	137 ± 7	118 ± 21	81 ± 7	82 ± 3

Evaluation of specific binding of [^{11}C]CPPC in control mice.

Brain regional distribution of [^{11}C]CPPC in normal control mice, dose escalation blocking study with unlabeled CPPC (Fig. S4). Male CD-1 mice (26-28 g, age = six to seven weeks) from Charles River Laboratories were used. The CPPC solution (0.3, 0.6, 1.2, 3.0, 10, and 20 mg/kg) was given IP 5 min before IV [^{11}C]CPPC, whereas baseline animals received vehicle (n = 5 per dose). Animals were sacrificed by cervical dislocation at 45 min following injection of 5.1 MBq (0.14 mCi) [^{11}C]CPPC [specific radioactivity = 511 GBq/µmol (13.8 Ci/µmol)] in 0.2 mL saline into a lateral tail vein. The whole brains were removed, weighed and their radioactivity content was determined in a γ-counter LKB/Wallac 1283 CompuGamma CS (Bridgeport, CT). The percentage of standardized uptake value (%SUV) was calculated.

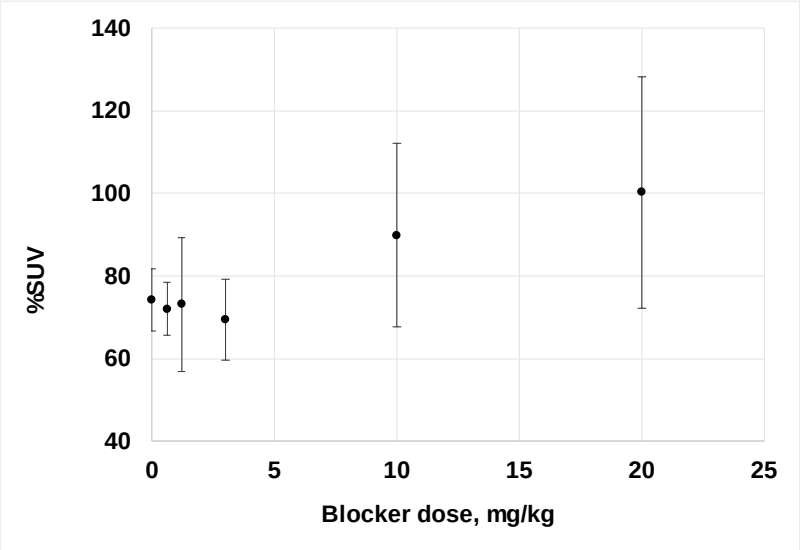

Figure S4. Blocking study with [^{11}C]CPPC and blocker CPPC. The study demonstrated an insignificant blockade with lower doses (0.6 – 3 mg/kg) and insignificant gradual increase of uptake with escalating doses (10-20 mg/kg) of unlabeled CPPC at time-point of 45 min after the tracer injection. Data: %SUV ± SD (n = 5)

Comparison of baseline and blocking uptake of [^{11}C]CPPC in the same experiment without and with blood correction (Fig. S5): Male CD-1 mice (25-27 g, age = six to seven weeks) from Charles River Laboratories were used. The CPPC solutions (0.6 or 3.0 mg/kg) was given IP 5 min before IV [^{11}C]CPPC, whereas baseline animals received vehicle (n = 3 per dose). Animals were sacrificed by cervical dislocation at 45 min following injection of 5.0 MBq (0.135 mCi) [^{11}C]CPPC [specific radioactivity = 390 GBq/µmol (10.5 Ci/µmol)] in 0.2 mL saline into a lateral tail vein. The brains were removed, cortex was rapidly dissected on ice and blood samples (0.2-0.5 cc) were taken from heart. The cortex and blood samples were weighed and their radioactivity content was determined in a γ-counter LKB/Wallac 1283 CompuGamma CS (Bridgeport, CT). The outcome variables for the cortex are presented without blood correction as %SUV (**Fig. S5A**) and with blood correction as SUVR (**Fig. S5B**).

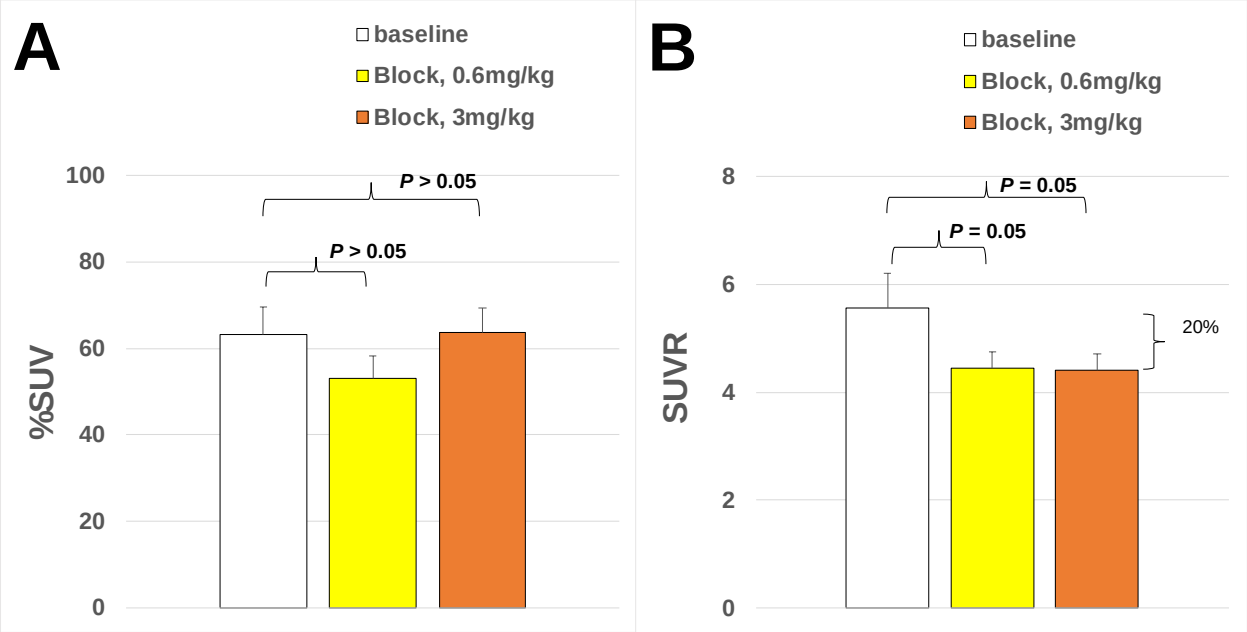

Figure S5. Comparison of baseline and blocking uptake of [^{11}C]CPPC in the cortex of CD1 mice in the same experiment without (Panel **A**) and with blood correction (Panel **B**). Panel **A**: mean %SUV ± SD (n = 3). No significant difference between the baseline and blocking with two doses of unlabeled CPPC (0.6 and 3 mg/kg) (P > 0.05). Panel **B**: Data: mean cortex SUVR ± SD (n =

3). In the mice injected with two doses of CPPC blocker, the blood corrected SUVR value was significantly lower (P = 0.05) than that in baseline (ANOVA). This experiment demonstrates that [^{11}C]CPPC specifically radiolabels CSF-1R in CD1 mouse brain cortex.

Brain uptake of [^{11}C]CPPC in the microglia-depleted and control mice (Fig. S6A): Male C57BL/6J mice (22-24 g) from Charles River Laboratories were purchased. Microglia-depleted mice were obtained by feeding the C57BL/6 mice (5 animals) for 3 weeks with pexidartinib (PLX3397)-formulated mouse chow (290 mg/kg) as described previously (4). The control C57BL/6J mice (5 animals) were fed with standard mouse chow for 3 weeks. On the last day of treatment, all animals were sacrificed by cervical dislocation at 45 min following injection of 5.0 MBq (0.135 mCi) [^{11}C]CPPC [specific radioactivity = 475 GBq/µmol (12.8 Ci/µmol)] in 0.2 mL saline into a lateral tail vein. The brains were removed, weighed and their radioactivity content was determined in a γ-counter LKB/Wallac 1283 CompuGamma CS (Bridgeport, CT). The outcome variables were calculated as %SUV.

Brain uptake of [^{11}C]CPPC in the CSF1R knock-out and control mice (Fig. S6B). Methods: B6.Cg-Csf1r$^{tm1.2Jwp}$/J (CSF1R knock-out, KO) mice (21-23 g; age = four to eight weeks; Jackson Laboratories, Bar Harbor, ME) (5 animals) and age-matched C57BL/6J controls (23-27 g) (5 animals) were used. The animals were injected IV with 3.7 MBq (0.1 mCi) [^{11}C]CPPC [specific radioactivity = 306 GBq/µmol (8.3 Ci/µmol)] and sacrificed by cervical dislocation at 45 min after the radiotracer injection. The whole brains were removed and blood samples (0.2-0.5 cc) were taken from heart. The whole brain and blood samples were weighed and their radioactivity content was determined in a γ-counter LKB/Wallac 1283 CompuGamma CS. The outcome variables were calculated as %SUV.

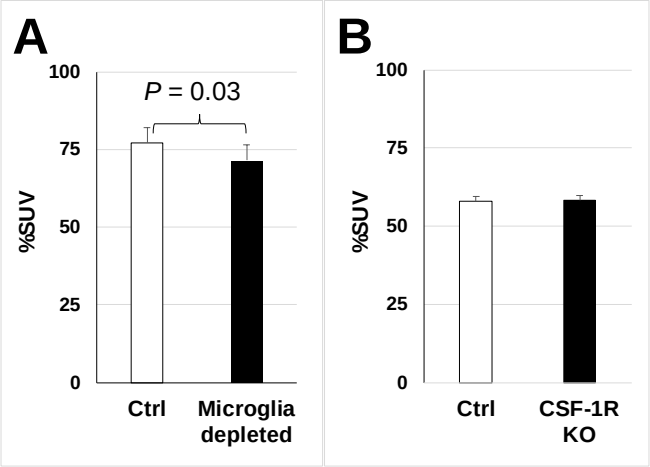

Figure S6. Comparison of whole brain uptake of [^{11}C]CPPC in control vs. microglia-depleted (Panel **A**) and control vs. CSF1R knock-out (Panel **B**) mice, 45 min after radiotracer injection. **A**: Data are mean %SUV ± SD (n = 5). **B**: Data are mean %SUV to blood ± SD (n = 5). Statistical analysis - ANOVA.

[^{11}C]CPPC brain uptake in the control and LPS - treated (intracranial) mice (Fig. 1):

Experiment 1, Fig. 1A. Nine male CD-1 mice (25-27 g, age = six to seven weeks) from Charles River Laboratories were divided in three cohorts: 1) sham-treated mice (n = 3), baseline; 2) lipopolysaccharide (LPS-intracranial) - treated mice (n = 3), baseline; and 3) lipopolysaccharide (LPS-intracranial) - treated mice (n = 3), blocking.

CD1 mice were anaesthetized with avertin (250 mg/kg, IP). Peri-procedural analgesia was provided with finadine (2.5 mg/kg, SC). The coordinates for intraparenchymal injection in the right forebrain were AP -0.5 mm' DV -2.5 mm; and ML 1.0 right of midline. The holes were drilled perpendicularly to the previously exposed skull. Sterile phosphate buffered saline (PBS) (0.5 µL) or 5 µg lipopolysaccharide (LPS, O11:B4, Calbiochem, San Diego, CA) in 0.5 µL PBS was injected into the brain parenchyma using a 1 µL Hamilton syringe. After injection, the needle was kept in the brain for additional 3 min and slowly removed. The incision was sealed with dental cement.

The radiotracer study was performed on the 3rd day after LPS administration. The CPPC solution (0.3 mg/kg) was given IP, 5 min before IV [^{11}C]CPPC, whereas baseline animals received vehicle. The LPS and control animals were injected IV with 3.7 MBq (0.1 mCi) [^{11}C]CPPC [specific radioactivity = 274 GBq/µmol (7.4 Ci/µmol)] and sacrificed by cervical dislocation at 45 min after the radiotracer injection. The whole brains were removed and dissected on ice. The cerebellum, ipsilateral brain hemisphere and contralateral brain hemisphere and blood samples were weighed and their radioactivity content was determined in a γ-counter LKB/Wallac 1283 CompuGamma CS. The outcome variables were calculated as %SUV.

Experiment 2, Fig. 1B. Sixteen male CD-1 mice (25-27 g, age = six to seven weeks) from Charles River Laboratories were divided in four cohorts: 1) sham-treated mice (n = 4), baseline; 2) lipopolysaccharide (LPS-intracranial) - treated mice (n = 4), baseline; 3) lipopolysaccharide (LPS-

intracranial) - treated mice (n = 4), blocking-0.6 mg/kg CPPC; 4) lipopolysaccharide (LPS-intracranial) - treated mice (n = 4), blocking-1.2 mg/kg CPPC.

The mice were anaesthetized with avertin (250 mg/kg, IP). Peri-procedural analgesia was provided with finadine (2.5 mg/kg, SC). The coordinates for intraparenchymal injection in the right forebrain were AP -0.5 mm' DV -2.5 mm; and ML 1.0 right of midline. The holes were drilled perpendicularly to the previously exposed skull. Sterile phosphate buffered saline (PBS) (0.5 µL) or 5 µg lipopolysaccharide (LPS, O11:B4, Calbiochem, San Diego, CA) in 0.5 µL PBS was injected into the brain parenchyma using a 1 µL Hamilton syringe. After injection, the needle was kept in the brain for additional 3 min and slowly removed. The incision was sealed with dental cement.

The radiotracer study was performed on the 3rd day after LPS administration. The CPPC solution (0.3 mg/kg) was given IP, 5 min before IV [^{11}C]CPPC, whereas baseline animals received vehicle. The LPS and control animals were injected IV with 3.7 MBq (0.1 mCi) [^{11}C]CPPC [specific radioactivity = 366 GBq/µmol (9.9 Ci/µmol)] and sacrificed by cervical dislocation at 45 min after the radiotracer injection. The whole brains were removed and dissected on ice. The cerebellum, the ipsilateral brain hemisphere that was further cut into two quadrants, frontal and caudal, and contralateral brain hemisphere and blood samples were weighed and their radioactivity content was determined in a γ-counter LKB/Wallac 1283 CompuGamma CS. The outcome variables were calculated as %SUV.

[^{11}C]CPPC brain uptake in the control and LPS - treated (intraperitoneal) mice (Fig. 2):

Experiment 1, Fig. 2A. Fifteen male CD-1 mice (25-27 g, age = six to seven weeks) from Charles River Laboratories were divided in three cohorts: 1) control mice (n = 5), baseline; 2) lipopolysaccharide (LPS) - IP treated (n = 5) mice, baseline; and 3) lipopolysaccharide (LPS) - IP treated (n = 5) mice, blocking with CPPC. The LPS (O111:B4, Calbiochem, San Diego, CA) solution in sterile saline (10 mg/kg, 0.2 mL) was administered intraperitoneally and the radiotracer study was performed on the 5th day after LPS administration. The CPPC solution (1 mg/kg) was given IP, 5 min before IV [^{11}C]CPPC, whereas baseline animals received vehicle.

The LPS and control animals were injected IV with 3.7 MBq (0.1 mCi) [^{11}C]CPPC [specific radioactivity = 444 GBq/µmol (12.0 Ci/µmol)] and sacrificed by cervical dislocation at 45 min after the radiotracer injection. The whole brains were removed and dissected on ice. The cerebellum and rest of brain were weighed and their radioactivity content was determined in a γ-counter LKB/Wallac 1283 CompuGamma CS. The outcome variables were calculated as %SUV.

Experiment 2, Fig. 2B. Fifteen male CD-1 mice (25-27 g, age = six to seven weeks) from Charles River Laboratories were divided in three cohorts: 1) control mice (n = 5), baseline; 2) lipopolysaccharide (LPS) - IP treated (n = 5) mice, baseline; and 3) lipopolysaccharide (LPS) - IP treated (n = 5) mice, blocking with CPPC. The LPS (O111:B4, Calbiochem, San Diego, CA) solution in sterile saline (10 mg/kg, 0.2 mL) was administered intraperitoneally and the radiotracer study was performed on the 3rd day after LPS administration. The CPPC solution (1 mg/kg) was given IP, 5 min before IV [^{11}C]CPPC, whereas baseline animals received vehicle.

The LPS and control animals were injected IV with 3.7 MBq (0.1 mCi) [^{11}C]CPPC [specific radioactivity = 374 GBq/µmol (10.1 Ci/µmol)] and sacrificed by cervical dislocation at 45 min after the radiotracer injection. The whole brains were removed and dissected on ice and blood samples (0.2-0.5 cc) were taken from heart. The whole brain and blood samples were weighed and their

radioactivity content was determined in a γ-counter LKB/Wallac 1283 CompuGamma CS. The outcome variables were calculated as SUVR.

Experiment 3, Fig. 2C. Fifteen male CD-1 mice (25-27 g, age = six to seven weeks) from Charles River Laboratories were divided in three cohorts: 1) control mice (n = 3), baseline; 2) lipopolysaccharide (LPS) - IP treated (n = 6) mice, baseline; and 3) lipopolysaccharide (LPS) - IP treated (n = 6) mice, blocking with compound 8. The LPS (O111:B4, Calbiochem, San Diego, CA) solution in sterile saline (10 mg/kg, 0.2 mL) was administered intraperitoneally and the radiotracer study was performed on the 3rd day after LPS administration. The compound 8 solution (2 mg/kg) was given IP, 5 min before IV [^{11}C]CPPC, whereas baseline animals received vehicle.

The LPS and control animals were injected IV with 3.0 MBq (0.08 mCi) [^{11}C]CPPC [specific radioactivity = 148 GBq/μmol (4.0 Ci/μmol)] and sacrificed by cervical dislocation at 45 min after the radiotracer injection. The whole brains were removed and dissected on ice and blood samples (0.2-0.5 cc) were taken from heart. The whole brain and blood samples were weighed and their radioactivity content was determined in a γ-counter LKB/Wallac 1283 CompuGamma CS. The outcome variables were calculated as SUVR to blood.

[^{11}C]CPPC brain uptake in the Alzheimer's mouse model and control mice (Fig. 3):

Mouse model of Alzheimer's disease-related amyloidosis overexpressed Amyloid Precursor Protein (APP) with Swedish and Indiana mutations was used. The transgenic APP had tetracycline transactivator (tTa) - sensitive promoter that was activated by over-expressing tTa driven by CaMKII promoter (5). Due to such combination of transgenes, the overexpression of transgenic APP was observed only in principal neurons of the forebrain. Mice that did not express any of the transgenes served as controls. The Alzheimer's male mice (AD) and their sex-matched control littermates were 16 months of age at the time of the study. At this age, the AD mice have significant Aβ amyloid plaque deposition in the forebrain including the cortex and hippocampus (5). Six AD mice and six age-matched controls were used for this study. The animals were injected IV with 5.6 MBq (0.15 mCi) [^{11}C]CPPC [specific radioactivity = 340 GBq/μmol (9.2 Ci/μmol)] and sacrificed by cervical dislocation at 45 min after the radiotracer injection. The whole brains were removed and rapidly dissected on ice. The cerebellum and rest of brain were weighed and their radioactivity content was determined in a γ-counter LKB/Wallac 1283 CompuGamma CS. The outcome variables were calculated as %SUV.

[^{11}C]CPPC full body radiation dosimetry in mice

Methods: Radiation dosimetry for [^{11}C]CPPC was studied in fifteen male CD-1 mice (23–27 g) following our published procedure (6). A solution of [^{11}C]CPPC in 0.2 ml of saline (7.4 MBq or 0.2 mCi) was injected as a bolus into the lateral tail vein, and groups of mice (n = 3) were euthanized at 10, 30, 45, 60, and 90 min after the radiotracer injection. The lungs, heart, kidneys, liver, spleen, intestine, stomach, and brain were quickly removed and put on ice. One femur and samples of thigh muscle, bone marrow and blood were also collected. The organs were weighed, and the tissue radioactivity was measured with an automated gamma counter (LKB Wallac 1282 CompuGamma CS Universal Gamma Counter). The percent injected dose per organ (%ID/organ) was calculated by comparison with samples of a standard dilution of the initial dose. All measurements were corrected for decay. Resultant values of %ID/organ were fit using the SAAM II software (7). Time integrals of activity (8) were entered into the OLINDA/EXM software (6), using the adult male model. Activity was observed in the intestines (~35%). The number of disintegrations in the remainder of body' was assumed to be equal to 100% of the activity administered integrated to total decay of ^{11}C, minus the disintegrations in other body organs.

Results: The fitted metabolic model, number of disintegrations in the source organs, and organ doses are summarized below:

The fitted metabolic model was as follows:

Organ	%	T-bio (hr)	%	T-bio (hr)
Brain	3.83	0.302	0.38	∞
Heart	1.00	0.272	0.14	∞
Lungs	8.27	0.159	1.53	2.27
Liver	97.6	0.764	-100	0.335
Kidneys	8.32	0.297	1.52	∞
Spleen	1.43	0.823	-1.24	0.145

The numbers of disintegrations in the source organs (in MBq-hr/MBq administered) were:

Brain	1.10E-02
LLI	7.00E-04
Small Intestine	1.53E-01
ULI	1.81E-02
Heart Wall	2.80E-03
Kidneys	2.65E-02
Liver	8.80E-02
Lungs	2.00E-02
Spleen	3.00E-03
Remainder	1.68E-01

The human radiation doses estimates are (adult male model):

Table S3. Estimated Human Doses.

Target Organ	mSv/MBq	rem/mCi
Adrenals	3.11E-03	1.15E-02
Brain	2.70E-03	9.99E-03
Breasts	1.29E-03	4.76E-03
Gallbladder Wall	5.35E-03	1.98E-02
LLI Wall	4.29E-03	1.59E-02
Small Intestine	4.73E-02	1.75E-01
Stomach Wall	2.76E-03	1.02E-02
ULI Wall	1.73E-02	6.42E-02
Heart Wall	3.72E-03	1.38E-02
Kidneys	2.56E-02	9.48E-02
Liver	1.60E-02	5.90E-02
Lungs	6.10E-03	2.26E-02
Muscle	1.84E-03	6.79E-03
Ovaries	5.21E-03	1.93E-02
Pancreas	3.18E-03	1.18E-02
Red Marrow	2.19E-03	8.09E-03
Osteogenic Cells	2.13E-03	7.87E-03
Skin	1.19E-03	4.41E-03
Spleen	6.08E-03	2.25E-02
Testes	1.20E-03	4.42E-03
Thymus	1.44E-03	5.33E-03
Thyroid	1.18E-03	4.38E-03
Urinary Bladder Wall	2.14E-03	7.92E-03
Uterus	4.57E-03	1.69E-02
Total Body	2.90E-03	1.07E-02
Effective Dose	4.80E-03	1.78E-02

Conclusion of radiation dosimetry study: The data were all well fit with two exponential functions. Most organs appear to receive around 0.002-0.006 mSv/MBq (0.007 to 0.011

rem/mCi). The small intestine appears to receive the highest dose, around 0.047 mSv/MBq (0.17 rem/mCi). The effective dose is about 0.0048 mSv/MBq (0.018 rem/mCi).

PET/CT imaging in mice with Experimental Autoimmune Encephalitis (Fig. 4, Fig. S7)

Adult female C57BL/6J mice, age = 13 weeks (Jackson Laboratories, Bar Harbor ME) were inoculated with MOG_{35-55} peptide and behaviorally scored as described previously (9): "Briefly, incomplete Freund's adjuvant (Pierce) containing 8 mg/ml of heat-killed Mycobacterium tuberculosis H37 RA (Difco) was mixed at 1:1 with a 2 mg/ml solution of MOG35-55 (Johns Hopkins Biosynthesis & Sequencing Facility): NH2-MEVGWYRSPFSRVVHLYRNGK-COOH diluted in phosphate-buffered saline (PBS). After forming a stable emulsion, a total of 100 µl of the resulting mixture was divided between two subcutaneous injection sites at the base of the tail (i.e. 400 µg of M. tuberculosis and 100 µg of MOG35-55 per mouse). On the day of immunization (day 0 post-immunization: day 0 p.i.) and 2 days later, 250 ng of pertussis toxin (EMD/Calbiochem, USA) diluted in PBS was injected intravenously."

Symptomatic MOG-inoculated mice and an un-inoculated, healthy mouse were scanned 14 days after the first inoculation. Scoring is determined according to (10). Briefly, mice are scored from 0-5, where a score of 0 represents no clinically observed features and a score of 5 represents complete hind limb paralysis with incontinence. A score of 3 represents moderate paraparesis with occasional tripping. Scores of 0.5 (distal limp tail), 2.5 (mild/moderate paraparesis with tripping) and 4.5 (complete hind limb paralysis) were assayed in this study. Each mouse was injected IV with 8.14 MBq [220 µCi, SA > 370 GBq/µmol (>10 Ci/µmol)] proceeded using a Sedecal SuperArgus PET/CT scanner (Madrid, Spain). CT scans for anatomic co-registration were performed over 512 slices at 60 kVp. PET and CT data were reconstructed using the manufacturer's software and displayed using AMIDE software (http://amide.sourceforge.net/). To preserve dynamic range, harderian and salivary gland PET signal was partially masked using a thresholding method (Fig. 4), whereas unmasked images are shown in Fig. S7. Regions of

interest were drawn over PET visible lesions through three slices and quantitated in the regions indicated.

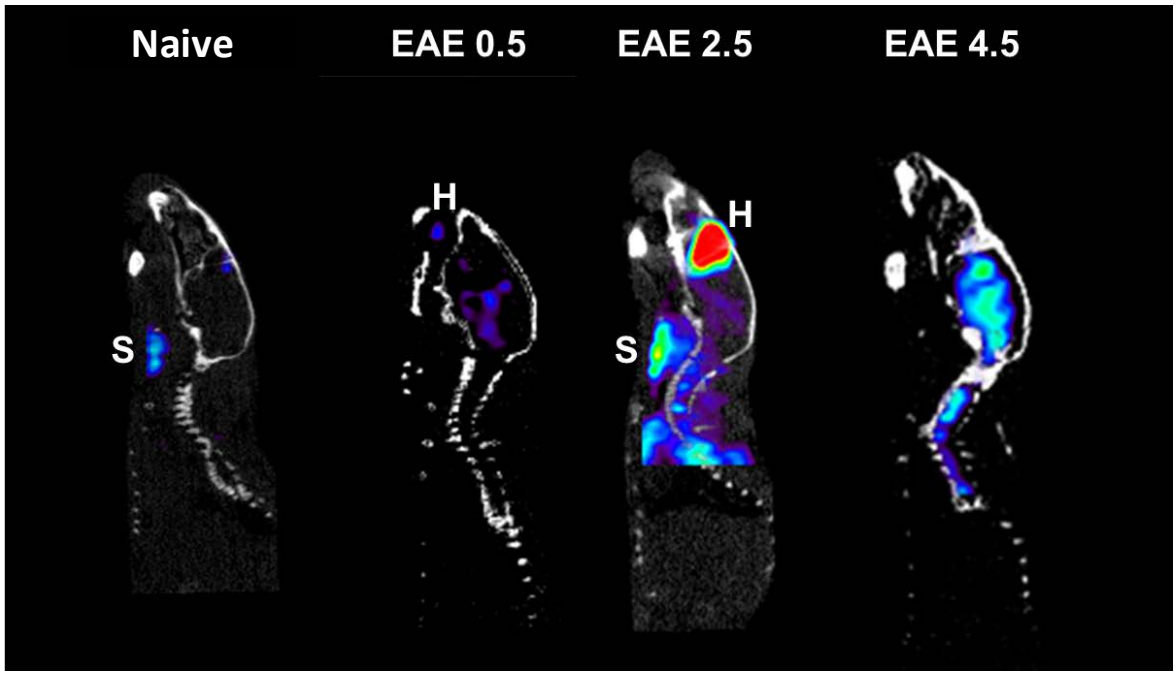

Figure S7. Sagittal slices of [^{11}C]CPPC PET/CT images in EAE mice with no thresholding. All images are scaled to the same maximum displayed in **Fig. 4**. S=salivary gland; H = Harderian gland

Mouse plasma and brain radiometabolite analysis

Six male CD-1 mice (25-27 g, age = six to seven weeks) from Charles River Laboratories were used. The animals were injected IV with 37 MBq (1 mCi) [^{11}C]CPPC [specific radioactivity = 673 GBq/μmol (18.2 Ci/μmol)] and sacrificed by cervical dislocation at 10 min (3 animals) and 30 min (3 animals) after the radiotracer injection. The whole brains were removed and dissected on ice and blood samples (0.5 cc) were taken from heart. Radiometabolites of [^{11}C]CPPC in the mouse plasma and brain were analyzed using a general HPLC method described above for baboon. Before the HPLC analysis the mouse brain was homogenized in 2 mL of mixture 50% acetonitrile : 50% phosphate buffer (Et_3N, H_3PO_4, pH 7.2). The homogenates were centrifuged (14000g for 5 min) and supernatants filtered using 0.2 micron filter and filtrate was analyzed by radio-HPLC with phenomenex Gemini C18, 10 μ, 4.6 x 250 mm and 2 mL/min isocratic elution and 50% acetonitrile - 50% aqueous triethylamine, c = 0.06 M and pH=7.2 as mobile phase. The study demonstrated that in mouse plasma the radiotracer [^{11}C]CPPC forms the same two radiometabolites as those in baboon plasma (Fig. S11). The radiometabolites poorly penetrate the blood-brain barrier and their presence in the brain is low (Table S4)

Table S4. Parent [^{11}C]CPPC and its radiometabolites in mouse plasma and brain.

Time-point	**Plasma**		**Brain**	
	Metabolites,%	Parent [^{11}C]CPPC, %	Metabolites,%	Parent [^{11}C]CPPC, %
10 min	29.9 ± 2.3	70.2 ± 2.2	3.4 ± 0.1	96.6 ± 0.1
30 min	60.3 ± 1.4	39.7 ± 1.3	4.9 ± 1.7	95.1 ± 1.6

Quantitative real time PCR (qRT-PCR) and western blot analyses of whole brain of control and LPS-treated CD1 mice.

Six male CD-1 mice (25-27 g, Charles River) were intraperitoneally injected with LPS (O111:B4, Calbiochem, San Diego, CA, 10 mg/kg, 0.2 mL). Mice were euthanized on day 4 post-LPS injection and whole brains were collected. Half of the brains were snap frozen in liquid nitrogen and stored at -80 °C for western blot analyses. The other half of brains were immediately stored in 1 mL of the RNA*later*® (Millipore Sigma, St. Luis, MO) at 4 °C. After 24 hr, RNA*later*® solution was removed from the samples and the brain was frozen at -80 °C for total RNA isolation.

Western Blot: For western blot, the brain samples were homogenized with T-PER Tissue Protein Extraction Reagent (Thermo Fisher Scientific, Halethorpe, MD) for 30 seconds total of 6 times and centrifuged at 12000 rpm for 5 min. Supernatant were collected and 10 µg of proteins were separated by SDS-PAGE and transferred onto the NC membrane. The following antibodies were used for Western blot analysis: α-mCSF1R Ab (Cell Signaling Technology, Danver, MA), α-mGAPDH Ab (Santa Cruz Biotechnology, Inc., Dallas, TX). The blots were visualized by Clarity Western ECL Substrate (Bio-Rad, Hercules, CA) and Gel Doc™ XR+ System (Bio-Rad). The band intensity was measured and calculated by Image Lab™ Software (Bio-Rad).

qRT-PCR: For qRT-PCR, total RNA was isolated from the brain using *Quick*-RNA™ Miniprep Kit, (Zymo Research, Irvine, CA) and cDNA were synthesized from the isolated RNA using High-capacity cDNA reverse transcription kit (Thermo Fisher Scientific). qPCR reactions were performed using the following Taqman™ assays: Csf1r: Mm01266652_m1, Pgk1: Mm00435617_m1, Gapdh: Mm99999915_g1). Relative quantity was calculated using Pgk1 and Gapdh as internal controls.

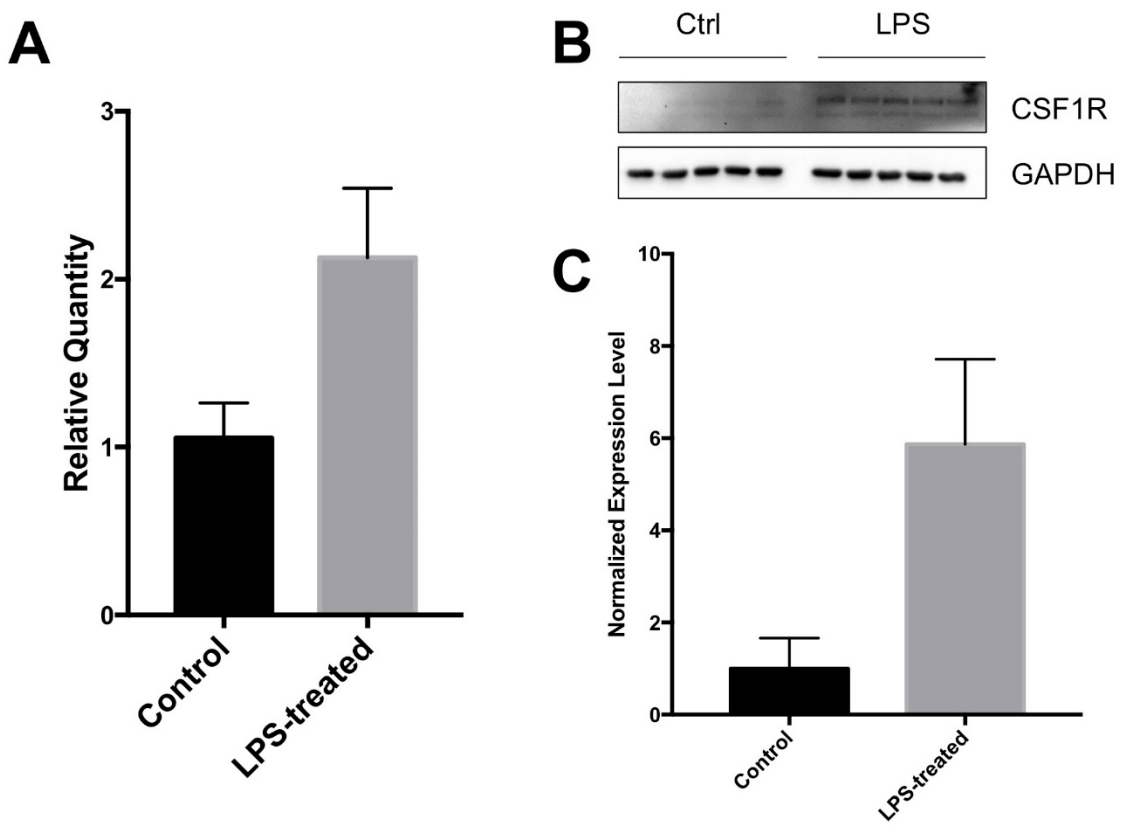

Figure S8. LPS treatment induced elevated expression of CSF1R in mouse brain. Panel **A**: Relative level of *Csf1r* mRNA measured by quantitative real time PCR (n=5). Panel **B**: Western blot analyses of total mouse brain extracts from control and LPS-treated mice brain. Each lane represents a mouse. Panel **C**: Band intensities of the CSF1R were calculated and normalized with those of GAPDH from panel B (n=5).

Baboon PET studies

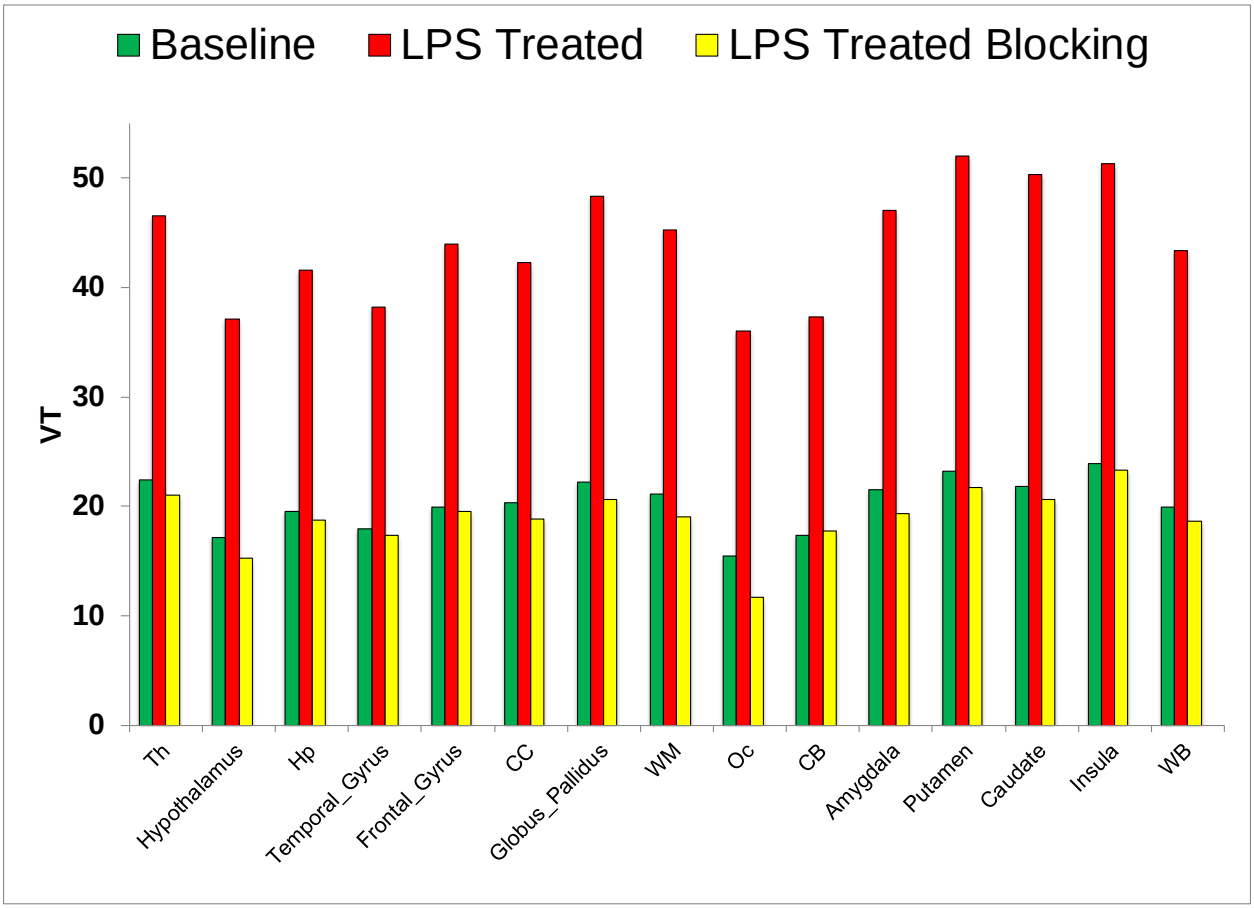

Figure S9. Regional V_T values of [^{11}C]CPPC in baseline (green), LPS-treated (red) and LPS plus blocker (yellow) baboon studies. Abbreviations: Th = thalamus; Hp = hippocampus; CC = corpus callosum; WM = white matter; Oc = occipital cortex; CB = cerebellum; Amyg = amygdala; WB = whole brain.

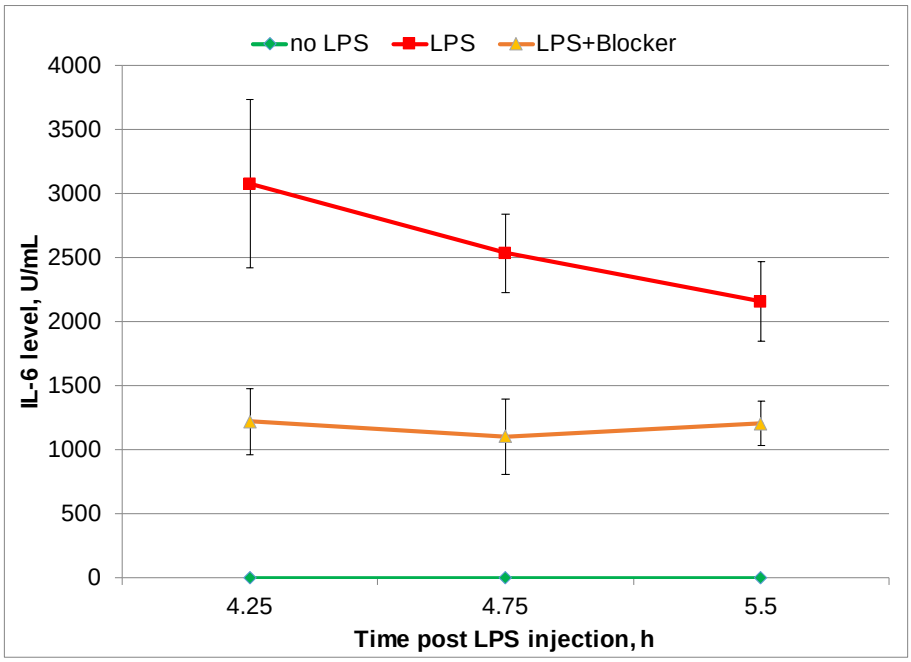

Figure S10. Levels of inflammatory cytokine IL-6 in baboon serum. The IL-6 level increased after the LPS injection and reduced in the LPS-plus-blocker study. IL-6 was measured with ELISA kit. Briefly: At three different time points (post injection 15, 45, and 90 minute), 2 mL of baboon peripheral blood was collected into BD Vacutainer (BD Biosciences, cat# 367983, La Jolla, CA) and centrifuged down at 2,000 x g for 10 min at room temperature. Serum was collected into sterile tubes and stored in -80°C for future immunoassay. Serum samples were thawed on ice and the IL-6 level was measured using IL-6 Monkey Instant ELISA™ (Thermo Fisher Scientific, cat# BMS641INST, Halethorpe, MD) according to the manufacturer's protocol.

Baboon Radiometabolite analysis

The relative percentage of [^{11}C]CPPC in plasma was determined by high performance liquid chromatography (HLPC) in blood samples drawn at 5, 10, 20, 30, 60, and 90 min after radiotracer injection. The modified column-switching HPLC method was used (Coughlin, NeuroImage 165, 2018, page 120). The HPLC system containing of a 1260 infinity quaternary pump, a 1260 infinity column compartment module, a 1260 infinity UV and a Raytest

GABI Star radiation detectors was operated with OpenLab CDS EZChrom (A.01.04) software. 0.4-1.5 mL of plasma samples loaded into a 2 mL Rheodyne injector loop were initially directed to the capture column (packed with Phenomenex Strata-X 33µm polymeric reversed phase sorbent) and both detectors with 1% acetonitrile and 99% water mobile phase at 2 mL/min. After 1 min of isocratic elution, analytical mobile phase composed of 65% acetonitrile and 35% aqueous solution triethylamine, c=0.06M and pH=7.2 (adjusted with phosphoric acid) was applied to direct trapped on the capture column non-polar compounds to an analytical column (Gemini C18(2) 10 µm 4.6x250 mm) and detectors at 2 mL/min. The HPLC system was standardized using non-radioactive CPPC and [^{11}C]CPPC prior to analysis of blood plasma samples, which were spiked with 5 µL of CPPC at concentration of 1 mg/mL. The total plasma time-activity curves were obtained by analyzing of 0.3 mL of blood plasma samples on a PerkinElmer Wizard 2480 automatic gamma counter. Plasma free fraction (fp) of [^{11}C]CPPC was determined using centrifree ultrafiltration devices.

Radiometabolite analysis was carried out using a column-switching HPLC method, which allows to inject blood plasma directly into HPLC system without time consuming prior protein precipitation and extraction. Initially sample is directed into capture column for solid phase extraction of parent tracer and its non-polar radiometabolites. Most of blood plasma constituents and polar radiometabolites of parent radiotracer do not retain on a capture column and are eluted into detectors. Then analytical mobile is applied to elute trapped compounds on the capture column into analytical column, where they are separated and further directed into detectors. This way all radioactive compounds present in the sample can be detected allowing for precise quantification of relative percentage of parent tracer versus its radiometabolites. As presented in the Fig. S11A, 100% of injected [^{11}C]CPPC could be effectively trapped on a capture column used and with analytical mobile phase it elutes at 7.35 min. Representative HPLC chromatogram of plasma samples obtained at different time intervals are presented in Fig. S11A and time dependent blood plasma relative percentage of [^{11}C]CPPC in non-treated control and LPS or LPS

+ blocking agent treated baboons is presented in the Fig. S11B. Administration of LPS or LPS and blocking agent did not affect metabolic pattern and rate of [^{11}C]CPPC. Two peaks at 0.97 min and 4.82 min of elution related to less lipophilic radiometabolite of parent tracer were detected. The relative percentage of [^{11}C]CPPC was 84.87 ±2.01, 75.57 ±1.76, 62.5 ±4.47, 51.73 ±6.14, 34.8 ±1.31 and 25.6 ±2.77 at 5, 10, 20, 30, 60, and 90 min post radiotracer injection.

Plasma free fraction of [^{11}C]CPPC determined using centrifree ultrafiltration devices was also not affected by LPS or LPS and blocking treatment and it was 5.48 ±0.98%.

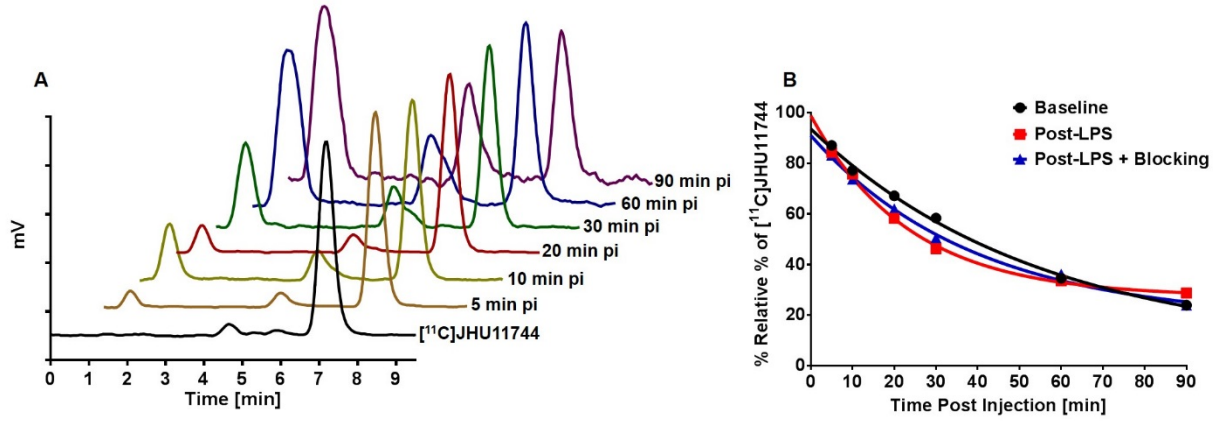

Figure S11. HPLC analysis of [^{11}C]CPPC ([^{11}C]JHU11744) radiometabolites in baboon plasma**.** Panel **A** - Radio-HPLC chromatograms of [^{11}C]CPPC and blood plasma sample collected at different time intervals, Panel **B** - time depended decrease of relative percentage of [^{11}C]CPPC in control and LPS or LPS and blocking agent treated baboons.

Baboon PET Imaging methods

PET images were acquired using a CPS/CTI High Resolution Research Tomograph (HRRT), which has an axial resolution (FWHM) of 2.4 mm, and in plane resolution of 2.4-2.8 mm. The animal was anesthetized and handled as described previously (11). The 90 min PET data were binned into 30 frames: four 15-sec, four 30-sec, three 1-min, two 2-min, five 4-min, and twelve 5-min frames. Images were reconstructed using the iterative ordered subset expectation maximization (OS-EM) algorithm (with six iterations and 16 subsets) with correction for radioactive decay, deadtime, attenuation, scatter and randoms(12). The reconstructed image space consisted of cubic voxels, each 1.22 mm^3 in size, and spanning dimensions of 31 cm x 31 cm (transaxially) and 25 cm (axially).

Blood samples were obtained via the arterial catheter at continually prolonged intervals throughout the 90 min scan (as rapidly as possible for the first 90 seconds, with samples acquired at increasingly longer intervals thereafter). Samples were centrifuged at 1,200 x g and the radioactivity in plasma were measured with a cross-calibrated gamma counter. Selected plasma samples (5, 10, 20, 30, 60, and 90 min) were analyzed with high performance liquid chromatography (HPLC) for radioactive metabolites in plasma as described above.

Baboon PET Data analysis

The image analysis and kinetic modeling were performed using software PMOD (v3.7, PMOD Technologies Ltd, Zurich, Switzerland). Dynamic PET images were first co-registered with the MRI images. A locally developed volume-of-interest (VOI) template, including 13 representative baboon brain structures, was then transferred to the animal's MRI image. The VOIs included frontal and temporal gyrus, thalamus, hippocampus, caudate, putamen, amygdala, globus

pallidus, insula, hypothalamus, cerebellum, corpus callosum, and white matter. Time activity curve (TAC) of each VOI was obtained by applying the VOI on PET frames.

Next, based on the TACs and the metabolite-corrected arterial plasma input functions, kinetic modeling was performed to quantitatively characterize the [^{11}C]CMPFF binding in brain. For brain uptake, the primary outcome measure is the regional brain distribution volume (V_T) of [^{11}C]CPPC, defined as concentration of the radiotracer in regional tissue relative to that in blood at equilibrium. Regional VT is proportional to the receptor density in the defined VOI. Because we don't anticipate any brain region to be devoid of specific [^{11}C]CPPC uptake, another commonly used outcome measure, namely, the non-displaceable binding potential (BPND), may not be obtained reliably.

For each VOI, VT was calculated using both compartmental modeling and the Logan graphical method(13). Time-consistency analysis was also performed. In Figure S12, we presented representative results. In summary, both compartmental modeling and Logan method are suitable for analyzing the [^{11}C]CPPC PET data (example shown in Fig. S12-a and b), and they generated very comparable regional VT results (Fig. S12-c). All brain regions yielded stable VT estimates for scan durations longer than 60 minutes (Fig. S12-d). To facilitate obtaining VT parametric images (Fig. 5 and Fig. S7), we chose the Logan method for presenting all VT values in the manuscript.

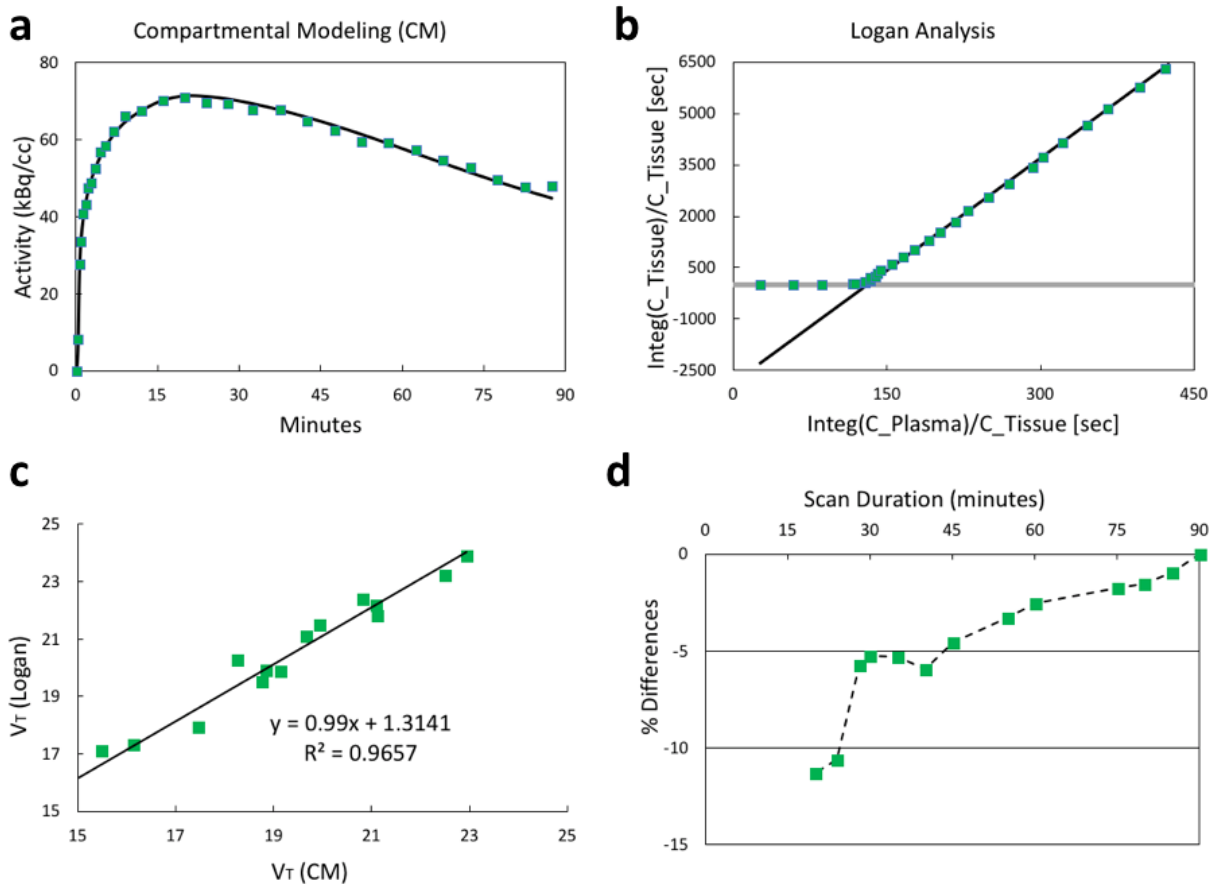

Figure S12. Representative plots of [^{11}C]CPPC kinetic analysis using (a) compartmental modeling and (b) Logan analysis, demonstrating both are suitable methods (representative region shown: putamen, green markers: PET study data points, solid lines: fitted data; (c) Comparisons of VT results by compartmental modeling and Logan analysis, in a representative baseline study, demonstrating they are highly comparable/correlated (R^2=0.9657); (d) Representative time-consistency plots of regional VT estimates (region: putamen), showing stable results (<2.5% changes) were obtained starting 60 min post injections.

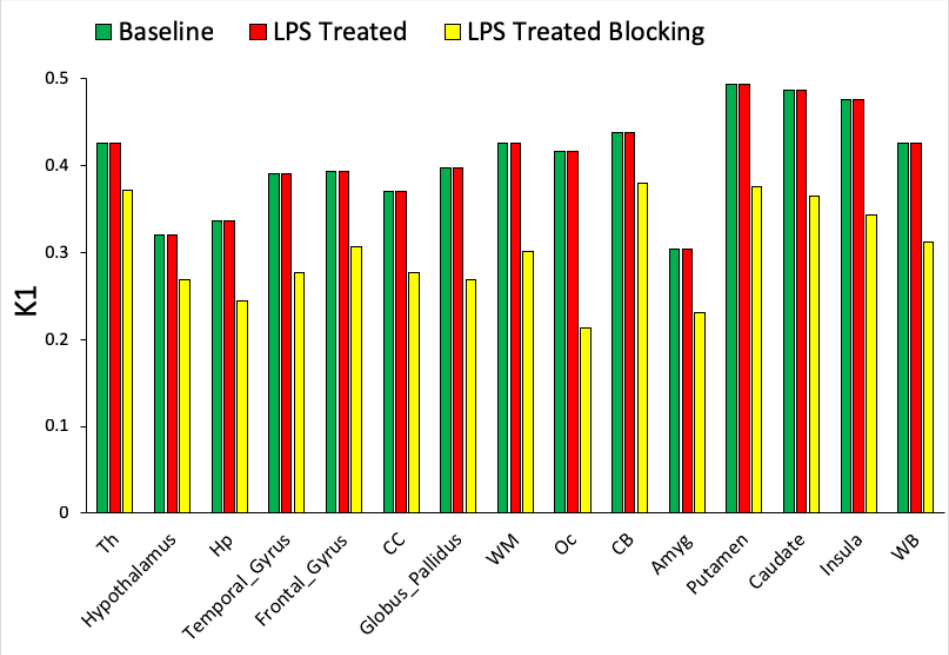

Figure S13. Regional K1 values of [^{11}C]CPPC in baseline (green), LPS-treated (red) and LPS plus blocker (yellow) baboon studies. Abbreviations: Th = thalamus; Hp = hippocampus; CC = corpus callosum; WM = white matter; Oc = occipital cortex; CB = cerebellum; Amyg = amygdala; WB = whole brain.

Post-mortem human brain autoradiography methods

Post-mortem inferior parietal cortex of three human subjects suffering from Alzheimer's disease and one healthy control (see Table S5 for demographics) was used for in vitro autoradiography. Human brain specimens were sectioned using a Microm HM550 cryomicrotome (Thermo-Fisher, Frederick, MD) to 20 µm thickness on charged glass slides. Two sections from each case were probed with 21 nM [^{11}C]CPPC (420 GBq/mmol (11,352 Ci/mmol)), while two additional sections from each case were probed with 21 nM radiotracer plus 2.74 µM of blocker (CPPC or PLX3397 or BLZ945 or compound 8) to test for target binding specificity (autoblockade). Binding took place in 100% fetal bovine serum (Sigma, St. Louis, MO) over 10 min at ambient temperature followed by two 5 min washes with 4°C PBS, pH 7.5. The slides were air dried and exposed to Kodak Biomax XAR film (Rochester, NY) for approximately 1 h prior to development and fixation using a Kodak X-O-Mat processor.

Quantification of in vitro binding densities from X-ray film: Films were digitized using a QICAM QIC-F-M-12 camera (Burnaby, BC, Canada) and Northern Light Illuminator and analyzed using MCID Core densitometry software (MCID, Cambridge, UK). Regions of interest (ROIs, white and gray matter) were identified by visual inspection of the sections and compared with serially diluted standards. The values are expressed as pmol/mm^3 of wet tissue ± standard deviation and reflect at least ten circular ROIs per region.

Table S5. Demographic data related to the post-mortem human brain tissue that was used in the autoradiography study.

Sample	Diagnosis	CERAD score	Braak score	Age	Sex	Race	Post-mortem delay, h
1-AD	Alzheimer's	C	6	88	F	white	8

2-AD	Alzheimer's	C	6	58	F	white	8.5
3-AD	Alzheimer's	C	6	61	M	white	13.5
4-Ctrl	Healthy control	n/a	n/a	48	F	black	12

Table S6. Autoradiography binding (pmol/mm^3) of [^{11}C]CPPC in the AD and healthy control post-mortem human brain slices (See also Fig. 7).

Sample	1-AD	2-AD	3-AD	4-control
Baseline	8.18 ± 0.68	7.20 ± 1.55	7.43 ± 1.59	4.11 ± 1.14
Blocking with unlabeled CPPC	4.72 ± 1.07	2.67 ± 0.53	3.73 ± 1.07	2.86 ± 1.06

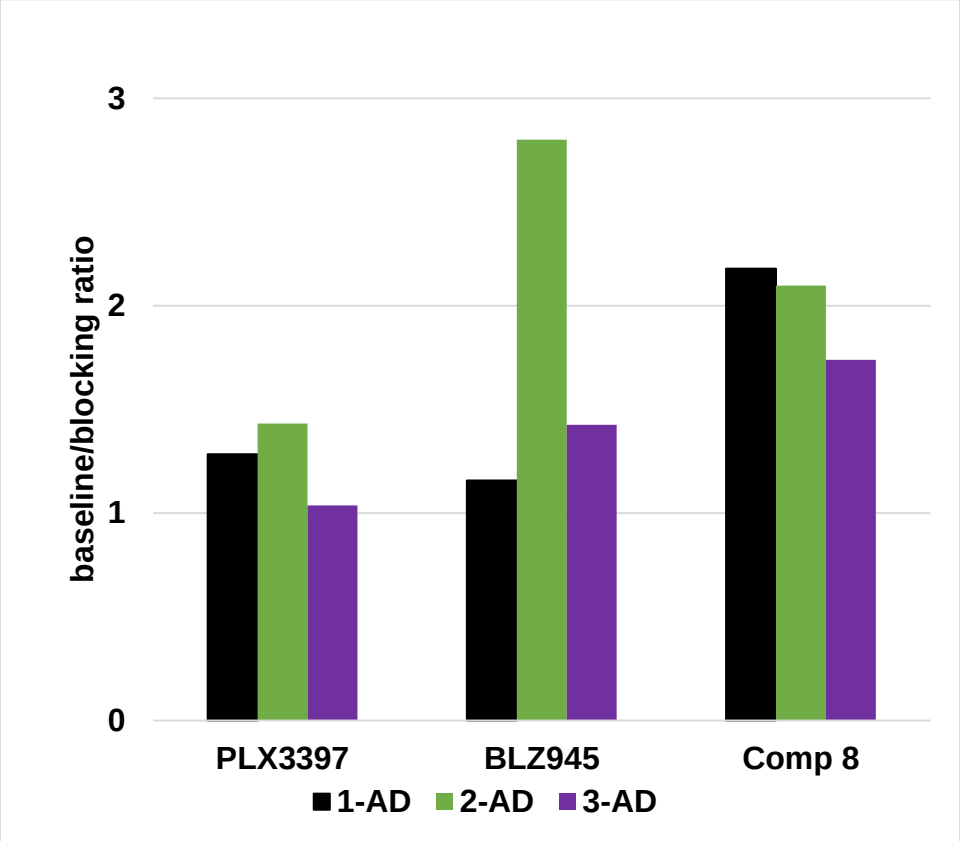

Figure S14. The baseline/blocking ratio with various blockers (PLX3397, BLZ945 and compound 8) in the autoradiography experiments with [^{11}C]CPPC in the AD post-mortem human brain slices.

Supporting Information References

1. Krauser JA*, et al.* (2015) Phenotypic and metabolic investigation of a CSF-1R kinase receptor inhibitor (BLZ945) and its pharmacologically active metabolite. *Xenobiotica* 45(2):107-123.
2. DeNardo DG*, et al.* (2011) Leukocyte complexity predicts breast cancer survival and functionally regulates response to chemotherapy. *Cancer Discov* 1(1):54-67.
3. Illig CR*, et al.* (2008) Discovery of novel FMS kinase inhibitors as anti-inflammatory agents. *Bioorg. Med. Chem. Lett.* 18(5):1642-1648.
4. Elmore MR*, et al.* (2014) Colony-stimulating factor 1 receptor signaling is necessary for microglia viability, unmasking a microglia progenitor cell in the adult brain. *Neuron* 82(2):380-397.
5. Melnikova T*, et al.* (2013) Reversible pathologic and cognitive phenotypes in an inducible model of Alzheimer-amyloidosis. *J. Neurosci.* 33(9):3765-3779.
6. Stabin MG, Sparks RB, & Crowe E (2005) OLINDA/EXM: the second-generation personal computer software for internal dose assessment in nuclear medicine. *J. Nucl. Med.* 46(6):1023-1027.
7. Foster DM (1998) Developing and testing integrated multicompartment models to describe a single-input multiple-output study using the SAAM II software system. *Adv Exp Med Biol* 445:59-78.
8. Stabin MG & Siegel JA (2003) Physical models and dose factors for use in internal dose assessment. *Health Phys.* 85(3):294-310.
9. Jones MV*, et al.* (2008) Behavioral and pathological outcomes in MOG 35-55 experimental autoimmune encephalomyelitis. *J. Neuroimmunol.* 199(1-2):83-93.
10. Beeton C, Garcia A, & Chandy KG (2007) Induction and clinical scoring of chronic-relapsing experimental autoimmune encephalomyelitis. *J Vis Exp* (5):224.
11. Horti AG*, et al.* (2016) 18F-FNDP for PET Imaging of Soluble Epoxide Hydrolase. *J. Nucl. Med.* 57(11):1817-1822.
12. Rahmim A, Cheng JC, Blinder S, Camborde ML, & Sossi V (2005) Statistical dynamic image reconstruction in state-of-the-art high-resolution PET. *Phys. Med. Biol.* 50(20):4887-4912.
13. Logan J*, et al.* (1990) Graphical analysis of reversible radioligand binding from time-activity measurements applied to [N-11C-methyl]-(-)-cocaine PET studies in human subjects. *J. Cereb. Blood Flow Metab.* 10(5):740-747.